

Lepton flavor violating Z -decays in supersymmetric seesaw model

J. Cao^{1,2}, Z. Xiong³, J.M. Yang^{2,4}

¹ CCAST (World Laboratory), P.O. Box 8730, Beijing 100080, P. R. China

² Institute of Theoretical Physics, Academia Sinica, Beijing 100080, P. R. China

³ Graduate School of Science, Hiroshima University, Hiroshima 937-6256, Japan

⁴ Department of Physics, Tohoku University, Aoba-ku, Sendai 980-8578, Japan

Received: 1 September 2003 /

Published online: 20 November 2003 – © Springer-Verlag / Società Italiana di Fisica 2003

Abstract. In the supersymmetric seesaw model, large flavor mixings of sleptons induce the lepton flavor violating (LFV) interactions $\ell_I \bar{\ell}_J V$ ($V = \gamma, Z$), which give rise to various LFV processes. In this work we examine the LFV decays $Z \rightarrow \ell_I \bar{\ell}_J$. Subject to the constraints from the existing neutrino oscillation data and the experimental bounds on the decays $\ell_J \rightarrow \ell_I \gamma$, these LFV Z -decays are found to be sizable, and among them the largest-rate channel $Z \rightarrow \tau \bar{\mu}$ can occur with a branching ratio of 10^{-8} and may be accessible at the LHC or GigaZ experiment.

1 Introduction

It is well known that the standard model (SM) predicts an unobservably small branching ratio for any lepton flavor violating (LFV) process, such as $\ell_J \rightarrow \ell_I \gamma$ or $Z \rightarrow \ell_I \bar{\ell}_J$. In some extensions of the SM the LFV processes may be significantly enhanced [1–3]. One example of these extensions is the popular weak-scale supersymmetry (SUSY). In SUSY models the LFV interactions $\ell_I \bar{\ell}_J V$ ($V = \gamma, Z$) [4–7] receive two kinds of additional loop contributions: One is from the charged-current lepton–neutrino–chargino couplings; the other is from the flavor mixings of charged sleptons. While the former is a common feature of all SUSY models accommodating right-handed neutrinos, the latter is sizable only in some specific realizations of SUSY, such as the minimal supergravity model (mSUGRA) [8] with the seesaw mechanism to generate the tiny masses for light neutrinos. This mechanism is realized by introducing right-handed neutrino superfields [1, 2] with very heavy Majorana masses. In such a framework the flavor diagonality of charged sleptons is usually assumed at the Planck scale, but the flavor mixings at the weak scale are inevitably generated through renormalization equations since there is no symmetry to protect the flavor diagonality. Such flavor mixings of charged sleptons generated at the weak scale are proportional to the neutrino Yukawa coupling, which may be as large as the top quark Yukawa coupling due to the seesaw mechanism, and they are enhanced by a large factor, $\log(M_P^2/\mathcal{M}^2)$ (M_P is the Planck scale and \mathcal{M} is the neutrino Majorana mass). Therefore, the popular mSUGRA with seesaw mechanism predicts large flavor mixings of sleptons at the weak scale, which will reveal their effects through some LFV processes in collider experiments.

The aim of this article is to examine the LFV Z -decays $Z \rightarrow \ell_I \bar{\ell}_J$ induced by slepton flavor mixings in the mSUGRA seesaw model. Given the possibility of the extremely accurate measurement of Z -decays in future experiments, the decays $Z \rightarrow \ell_I \bar{\ell}_J$ may serve as a sensitive probe for such a new physics model.

We will use the existing neutrino oscillation data and the experimental bounds on the decay $\ell_J \rightarrow \ell_I \gamma$ to constrain the model parameters, and then evaluate the branching ratios of $Z \rightarrow \ell_I \bar{\ell}_J$. We find that, subject to the current constraints, the channel $Z \rightarrow \tau \bar{\mu}$ can occur with a branching ratio as large as 10^{-8} and thus may be accessible at LHC [9] or the GigaZ option of TESLA at DESY [10].

This article is organized as follows. In Sect. 2, we briefly describe the SUSY seesaw model with *minimal CP*-violation in the right-hand neutrino sector and discuss the induced flavor mixings between sleptons. In Sect. 3, we present the analytic results for the SUSY contributions to the branching ratio of $Z \rightarrow \ell_I \bar{\ell}_J$. In Sect. 4, we present the correlation between the process $Z \rightarrow \ell_I \bar{\ell}_J$ and $\ell_J \rightarrow \ell_I \gamma$. In Sect. 5, we evaluate the numerical size of the branching ratio of $Z \rightarrow \ell_I \bar{\ell}_J$. Finally, in Sect. 6, we give our conclusions.

2 Supersymmetric seesaw model and charged slepton mixings

2.1 Supersymmetric seesaw model

The seesaw mechanism [11] provides an elegant explanation for the tiny masses of light neutrinos, which implies that the new physics scale is about 10^{14} GeV. However, a

non-symmetric seesaw model suffers from a serious hierarchy problem [1], which can be automatically solved in the SUSY framework.

In the supersymmetric seesaw model with N right-handed neutrino singlet fields ν_R , additional terms in the superpotential arise [1]:

$$W_\nu = -\frac{1}{2}\nu_R^{cT}\mathbf{M}\nu_R^c + \nu_R^{cT}\mathbf{Y}_\nu L \cdot H_2, \quad (1)$$

where \mathbf{M} is an $N \times N$ mass matrix for the right-handed neutrino, and L and H_2 denote the left-handed lepton and the Higgs doublet with hypercharge -1 and $+1$, respectively. At energies much below the mass scale of the right-handed neutrinos, the superpotential leads to the following mass matrix for the left-handed neutrinos:

$$\mathbf{M}_\nu = \mathbf{m}_D^T \mathbf{M}^{-1} \mathbf{m}_D = \mathbf{Y}_\nu^T \mathbf{M}^{-1} \mathbf{Y}_\nu (v \sin \beta)^2. \quad (2)$$

Obviously, the neutrino masses tend to be light if the mass scale \mathcal{M} of the matrix \mathbf{M} is much larger than the scale of the Dirac mass matrix $\mathbf{m}_D = \mathbf{Y}_\nu \langle H_2^0 \rangle = \mathbf{Y}_\nu v \sin \beta$ with $v = 174$ GeV and $\tan \beta = \langle H_2^0 \rangle / \langle H_1^0 \rangle$. The matrix \mathbf{M}_ν can be diagonalized by the MNS matrix \mathbf{U}_ν :

$$\mathbf{U}_\nu^\dagger \mathbf{M}_\nu \mathbf{U}_\nu^* = \text{diag}(m_{\nu 1}, m_{\nu 2}, m_{\nu 3}), \quad (3)$$

where $m_{\nu i}$ are the light neutrino masses.

2.2 Slepton flavor mixings

The mass matrix of the charged sleptons is given by

$$\mathbf{m}_\ell^2 = \begin{pmatrix} \mathbf{m}_{\ell LL}^2 & \mathbf{m}_{\ell LR}^{2\dagger} \\ \mathbf{m}_{\ell LR}^2 & \mathbf{m}_{\ell RR}^2 \end{pmatrix}, \quad (4)$$

with

$$\mathbf{m}_{\ell LL}^2 = \mathbf{m}_L^2 + \left[m_\ell^2 + m_Z^2 \left(-\frac{1}{2} + s_W^2 \right) \cos 2\beta \right] \mathbf{1}, \quad (5)$$

$$\mathbf{m}_{\ell RR}^2 = \mathbf{m}_R^2 + (m_\ell^2 - m_Z^2 s_W^2 \cos 2\beta) \mathbf{1}, \quad (6)$$

$$\mathbf{m}_{\ell LR}^2 = \mathbf{A}_\ell v \cos \beta - m_\ell \mu \tan \beta \mathbf{1}, \quad (7)$$

where $s_W = \sin \theta_W$, $c_W = \cos \theta_W$, θ_W is the Weinberg angle and $\mathbf{1}$ is the unit 3×3 matrix in generation space. In the mSUGRA model it is assumed that at the Planck scale the soft-breaking parameters satisfy

$$\mathbf{m}_{\tilde{L}} = \mathbf{m}_{\tilde{R}} = \mathbf{m}_{\tilde{\nu}} = m_0 \mathbf{1}, \quad m_{H_1} = m_{H_2} = m_0, \quad (8)$$

$$\mathbf{A}_\ell = A_0 \mathbf{Y}_\ell, \quad \mathbf{A}_\nu = A_0 \mathbf{Y}_\nu.$$

In general, the lepton Yukawa couplings \mathbf{Y}_ℓ and \mathbf{Y}_ν cannot be diagonalized simultaneously. It is usually assumed that \mathbf{Y}_ℓ is flavor diagonal but \mathbf{Y}_ν is not. In this basis the mass matrix of the charged sleptons is flavor diagonal at the Planck scale. However, when evolving down through the renormalization group (RG) equations (see Appendix A)

to the weak scale, such flavor diagonality is broken. In the leading-log approximation, we have [2]

$$\delta(\mathbf{m}_L^2)_{IJ} \simeq -\frac{1}{8\pi^2} (3m_0^2 + A_0^2) (\mathbf{Y}_\nu^{0\dagger} \mathbf{Y}_\nu^0)_{IJ} \ln \left(\frac{M_P}{\mathcal{M}} \right), \quad (9)$$

$$\delta(\mathbf{m}_R^2)_{IJ} \simeq 0, \quad (10)$$

$$\delta(\mathbf{A}_\ell)_{IJ} \simeq -\frac{3}{16\pi^2} A_0 (\mathbf{Y}_\ell^0)_{II} (\mathbf{Y}_\nu^{0\dagger} \mathbf{Y}_\nu^0)_{IJ} \ln \left(\frac{M_P}{\mathcal{M}} \right), \quad (11)$$

where $\mathbf{Y}^0 \equiv \mathbf{Y}(M_P)$.

The flavor non-diagonal mass matrix \mathbf{m}_ℓ^2 in (4) at the weak scale can be diagonalized by a unitary matrix \mathbf{S}_ℓ ,

$$\mathbf{S}_\ell \mathbf{m}_\ell^2 \mathbf{S}_\ell^\dagger = \text{diag}(m_{\ell X}^2). \quad (12)$$

Such a unitary rotation of slepton fields is to induce the flavor-changing neutral-current vertices: $\tilde{\chi}_\alpha^0 \ell_I \tilde{\ell}_X$ and $Z \tilde{\ell}_X \tilde{\ell}_Y$.

In the supersymmetric seesaw model, there exist right-handed sneutrinos with masses of the same order as the heavy Majorana neutrinos. However, due to their large masses, they do not give significant contributions to the considered LFV processes. Therefore, only the left-handed sneutrinos need to be taken into account, whose mass matrix is given by

$$\mathbf{m}_\nu^2 = \mathbf{m}_L^2 + \frac{1}{2} m_Z^2 \cos 2\beta \mathbf{1}. \quad (13)$$

Due to the non-diagonal contribution $\delta(\mathbf{m}_L^2)_{IJ}$ in (9), \mathbf{m}_ν^2 is flavor non-diagonal at the weak scale and needs to be diagonalized by a unitary matrix \mathbf{S}_ν ,

$$\mathbf{S}_\nu \mathbf{m}_\nu^2 \mathbf{S}_\nu^\dagger = \text{diag}(m_{\nu X}^2). \quad (14)$$

Such a unitary rotation of sneutrino fields results in the charged-current flavor-changing vertex $\tilde{\chi}_\alpha^+ \ell_I \tilde{\nu}_X$.

2.3 The form of the neutrino Yukawa coupling

As shown in (9) and (11), the flavor mixings of charged sleptons are proportional to the neutrino Yukawa couplings. Lack of knowledge of the neutrino Yukawa couplings results in numerous speculations on their possible forms. Different forms may lead to different flavor mixings. In this work we consider a scenario called the *minimal CP*-violating seesaw model which has two heavy Majorana neutrinos with the Dirac mass matrix \mathbf{m}_D parameterized as [12]

$$\mathbf{m}_D^T \equiv \mathbf{Y}_\nu^T \langle H_2^0 \rangle = \mathbf{U}_L \mathbf{m} \mathbf{V}_R, \quad \mathbf{m} = \begin{pmatrix} 0 & 0 \\ m_2 & 0 \\ 0 & m_3 \end{pmatrix}, \quad (15)$$

where

$$\mathbf{V}_R = \begin{pmatrix} \cos \theta_R & \sin \theta_R \\ -\sin \theta_R & \cos \theta_R \end{pmatrix} \begin{pmatrix} e^{-i\gamma_R/2} & 0 \\ 0 & e^{i\gamma_R/2} \end{pmatrix}, \quad (16)$$

with mixing angle θ_R and CP -violating phase γ_R for the heavy Majorana neutrinos directly concerned with leptogenesis [12]. The matrix \mathbf{U}_L appearing in (15) reads

$$\mathbf{U}_L = \mathbf{O}_{23}(\theta_{L23})\mathbf{U}_{12}(\theta_{L13}, \delta_L)\mathbf{O}_{12}(\theta_{L12})\mathbf{P}(-\gamma_L/2), \quad (17)$$

where $\mathbf{P}(-\gamma_L/2) = \text{diag}[1, \exp(-i\gamma_L/2), \exp(i\gamma_L/2)]$, and \mathbf{O}_{ij} and \mathbf{U}_{ij} denote rotations in the (i, j) plane. Without loss of generality, the $m_{2,3}$ in (15) are chosen to be real, positive and $m_2 < m_3$.

As (2) and (15) are used, the mass matrix for the light neutrinos in this model can be further expressed as

$$\mathbf{M}_\nu = \mathbf{U}_L \mathbf{m} \mathbf{V}_R \mathbf{M}^{-1} \mathbf{V}_R^T \mathbf{m}^T \mathbf{U}_L^T. \quad (18)$$

The MNS matrix in (3) is found to be a product of matrices,

$$\mathbf{U}_\nu = \mathbf{U}_L \mathbf{K}_R, \quad (19)$$

where $\mathbf{K}_R = \mathbf{K}_R(\theta, \phi, \alpha)$ is a unitary matrix. Therefore, (3) can be rewritten as

$$\mathbf{K}_R^\dagger \mathbf{m} \mathbf{V}_R \mathbf{M}^{-1} \mathbf{V}_R^T \mathbf{m}^T \mathbf{K}_R^* = \text{diag}[m_{\nu_1}, m_{\nu_2}, m_{\nu_3}]. \quad (20)$$

From this equation, one can learn that both \mathbf{K}_R and m_{ν_i} are independent of the choice of \mathbf{U}_L .

It is noticeable that the special form (15) for the neutrino Yukawa couplings matrix \mathbf{Y}_ν implies [12] the following.

- (1) One of the neutrinos is massless, i.e., $m_{\nu_1} = 0$.
- (2) The quantity $\mathbf{Y}_\nu^\dagger \mathbf{Y}_\nu$ is only dependent on the three mixing angles $\theta_{L12, L13, L23}$ and a CP -violating phase δ_L in \mathbf{U}_L ,

$$(\mathbf{Y}_\nu^\dagger \mathbf{Y}_\nu)_{IJ} = \frac{m_2^2 (\mathbf{U}_L)_{I2} (\mathbf{U}_L^\dagger)_{2J} + m_3^2 (\mathbf{U}_L)_{I3} (\mathbf{U}_L^\dagger)_{3J}}{(v \sin \beta)^2}. \quad (21)$$

- (3) For small mixing angles θ_{L13} and θ , the light neutrinos mixing matrix \mathbf{U}_ν takes a simplified form similar to the mixing matrix introduced in [13]:

$$\mathbf{U}_\nu \simeq \begin{pmatrix} c_{L12} & s_{L12} & s_{L13} e^{-i\delta_L} \\ -s_{L12} c_{L23} & c_{L12} c_{L23} & +s_{L12} s_\theta e^{-i\phi'} \\ s_{L12} s_{L23} & -c_{L12} s_{L23} & s_{L23} \end{pmatrix} \mathbf{P}(\alpha'), \quad (22)$$

where $\phi' = \phi + \gamma_L$, $\alpha' = \alpha - \gamma_L/2$ and $s_x \equiv \sin x$, $c_x \equiv \cos x$. In this case, the angles in $\mathbf{Y}_\nu^\dagger \mathbf{Y}_\nu$ can be related directly to the corresponding neutrino mixing angles and determined by neutrino experiments.

3 The LFV decays $Z \rightarrow \ell_I \bar{\ell}_J$

The flavor-changing interactions in the slepton sector discussed in the preceding section, namely the couplings $\tilde{\chi}_\alpha^0 \ell_I \bar{\ell}_J$ and $Z \tilde{\ell}_I \bar{\ell}_J$ from charged slepton mixings as well as $\tilde{\chi}_\alpha^\pm \ell_I \tilde{\nu}_J$ from sneutrino mixings, can induce the LFV processes $Z \rightarrow \ell_I \bar{\ell}_J$, as shown in Fig. 1. The relevant Feynman rules can be derived straightforwardly from the analysis

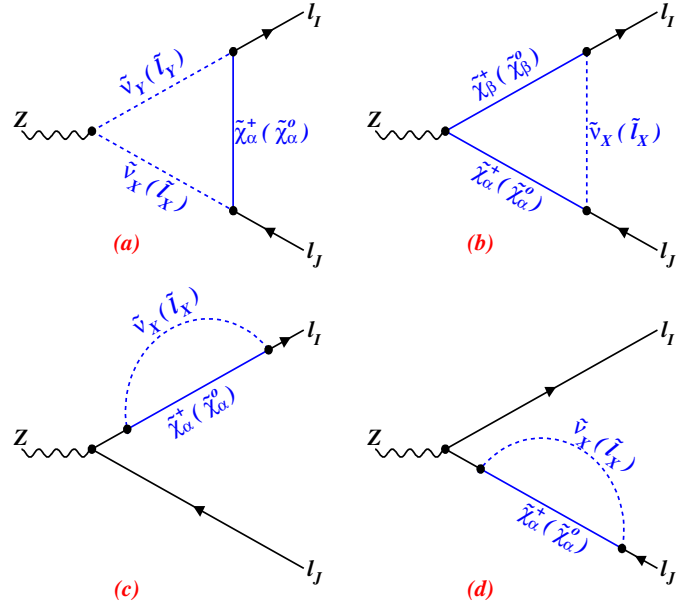


Fig. 1a–d. Feynman diagrams of SUSY contributions to the LFV processes $Z \rightarrow \ell_I \bar{\ell}_J$

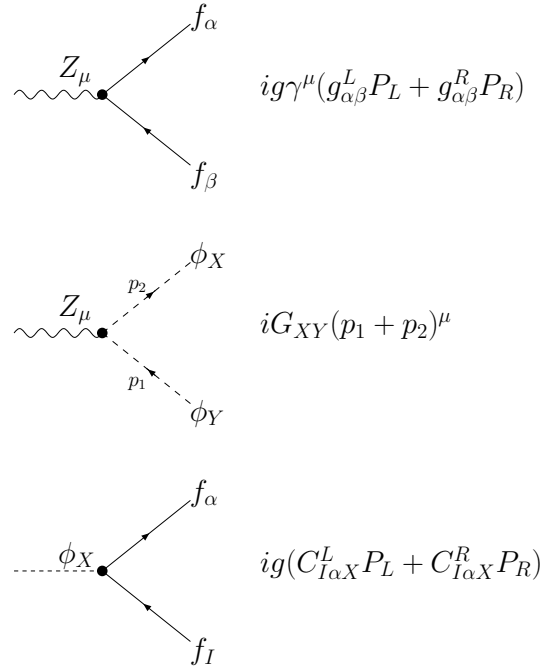


Fig. 2. Some interaction vertices needed to calculate the branching ratio of $Z \rightarrow \ell_I \bar{\ell}_J$ in SUSY. α and β are indices of charginos (neutralinos), while X and Y are those for sleptons

in the preceding section. Our analytic results will be expressed in terms of the constants $g_{\alpha\beta}^{L,R}$, G_{XY} and $C_{I\alpha X}^{L,R}$ defined in Fig. 2, whose explicit expressions can be found in [7, 14]. The calculation of the diagrams in Fig. 1 results in an effective $Z \ell_I \bar{\ell}_J$ vertex:

$$\mathcal{M} = i g \epsilon_\mu \bar{u}_{\ell_I}(p_1) \Gamma^\mu u_{\ell_J}(p_2), \quad (23)$$

with ε_μ being the polarization vector of Z -boson, $p_1(p_2)$ the momentum of $\ell_I(\ell_J)$, and Γ^μ given by

$$\Gamma^\mu = \frac{\alpha_{\text{em}}}{\sin^2 \theta_W} \quad (24)$$

$$\times [\gamma^\mu (f_{1L} P_L + f_{1R} P_R) + i\sigma^{\mu\nu} k_\nu (f_{2L} P_L + f_{2R} P_R)],$$

where $P_{R,L} = \frac{1}{2}(1 \pm \gamma_5)$, $g = e/\sin \theta_W$ and $k = p_1 - p_2$ is the momentum transfer. The form factors f_{1L} , f_{1R} , f_{2L} and f_{2R} arising from the calculation of the loop diagrams in Fig. 1 are listed as follows.

Contribution of Fig. 1a.

$$f_{1L}^a = G_{XY} C_{I\alpha X}^{*L} \quad (25)$$

$$\times [-2C_{24}^a C_{J\alpha Y}^L + m_{\ell_J} m_\alpha (C_0^a + C_{11}^a + C_{12}^a) C_{J\alpha Y}^L],$$

$$f_{2L}^a = G_{XY} C_{I\alpha X}^{*R} \quad (26)$$

$$\times [m_\alpha (C_0^a + C_{11}^a + C_{12}^a) C_{J\alpha Y}^L$$

$$- m_{\ell_J} (C_{12}^a + C_{22}^a + C_{23}^a) C_{J\alpha Y}^R].$$

Contribution of Fig. 1b.

$$f_{1L}^b = C_{I\alpha X}^{*L} C_{J\beta X}^L$$

$$\times \left[g_{\alpha\beta}^L m_\alpha m_\beta C_0^b + g_{\alpha\beta}^R \left(m_Z^2 C_{23}^b - 2C_{24}^b + \frac{1}{2} \right) \right]$$

$$+ C_{I\alpha X}^{*L} C_{J\beta X}^R g_{\alpha\beta}^L m_\alpha m_{\ell_J} (C_0^b + C_{11}^b + C_{12}^b), \quad (27)$$

$$f_{2L}^b = C_{I\alpha X}^{*R} C_{J\beta X}^L (g_{\alpha\beta}^R m_\alpha C_{11}^b + g_{\alpha\beta}^L m_\beta C_{12}^b)$$

$$+ C_{I\alpha X}^{*R} C_{J\beta X}^R g_{\alpha\beta}^L m_{\ell_J} (C_{12}^b + C_{22}^b + C_{23}^b). \quad (28)$$

Contribution of Fig. 1c,d.

$$f_{1L}^c = C_{I\alpha X}^{*L} \left[\frac{m_\alpha}{m_J} (B_0^1 - B_0^2) C_{J\alpha X}^{*R} - B_1^1 C_{J\alpha X}^L \right] g_L, \quad (29)$$

$$f_{1R}^c = 0. \quad (30)$$

In the above, $g_L = (1 - 2\sin^2 \theta_W)/(2\cos \theta_W)$, and $B_{0,1}^i = B(-p_i; m_\alpha^2, m_X^2)$, $C_{0,ij}^a = C_{0,ij}(-p_1, -p_2; m_\alpha^2, m_Y^2, m_X^2)$ and $C_{0,ij}^b = C_{0,ij}(-p_1, -p_2; m_X^2, m_\beta^2, m_\alpha^2)$ are the Feynman loop integral functions [15]. Terms proportional to the lepton masses m_{ℓ_I} are neglected. The right-handed form factors from the vertex loops are obtained from the corresponding left-handed ones in (25)–(28) by the substitution $L \leftrightarrow R$.

The branching ratio of $Z \rightarrow \ell_I \bar{\ell}_J$ (including its charge-conjugate channel) is then given by¹

$$\mathcal{B}r(Z \rightarrow \ell_I \bar{\ell}_J) = \frac{1}{48\pi^2} \left(\frac{\alpha_{\text{em}}}{\sin^2 \theta_W} \right)^3 \quad (31)$$

$$\times \frac{m_Z}{\Gamma_Z} \left[|f_{1L}|^2 + |f_{1R}|^2 + \frac{m_Z^2}{2} (|f_{2L}|^2 + |f_{2R}|^2) \right],$$

¹ Our result is in agreement with that given in [7] if m_{ℓ_J} -dependence terms in $f_{1L,1R}$ are neglected

where $f_{iL,iR} = \sum_{\alpha=a,b,c} f_{iL,iR}^\alpha$ and Γ_Z denotes the total decay width of the Z -boson.

Although the above results are sufficient to allow for numerical calculations, we would like to derive an analytical expression for the branching ratio by considering the limit $m_S \gg m_Z$ where m_S represents the mass of any internal sparticle in the loops in Fig.1. In this case the loop functions can be much simplified and we use the mass-insertion approximation in our derivation. In such a limit, the chargino mass matrix

$$\mathbf{M}_{\tilde{\chi}^\pm} = \begin{pmatrix} M_2 & \sqrt{2}m_W \sin \beta \\ \sqrt{2}m_W \cos \beta & \mu \end{pmatrix} \quad (32)$$

is nearly diagonal. Here μ is the mass parameter appearing in the term $\mu H_1 H_2$ in the superpotential and M_2 is the $SU(2)$ gaugino mass parameter. The matrices \mathbf{U} and \mathbf{V} which diagonalize $\mathbf{M}_{\tilde{\chi}^\pm}$ will be the unit ones for $\mu > 0$, and the chargino masses are given by

$$m_{\tilde{\chi}_1^\pm} = M_2, \quad m_{\tilde{\chi}_2^\pm} = |\mu|. \quad (33)$$

The symmetric neutralino mass matrix

$$\mathbf{M}_{\tilde{\chi}^0} = \begin{pmatrix} M_1 & & & \\ & M_2 & & \\ -m_Z s_W c_\beta & m_Z c_W c_\beta & & 0 \\ m_Z s_W s_\beta & -m_Z c_W s_\beta & -\mu & 0 \end{pmatrix} \quad (34)$$

can be diagonalized by a unitary matrix \mathbf{N} ,

$$\mathbf{N} = \begin{pmatrix} 1 & & & \\ & 1 & & \\ & & \sqrt{2}e^{i\frac{\pi}{4}} & -\sqrt{2}e^{-i\frac{\pi}{4}} \\ & & -\sqrt{2}e^{-i\frac{\pi}{4}} & \sqrt{2}e^{i\frac{\pi}{4}} \end{pmatrix}. \quad (35)$$

The corresponding mass eigenvalues are given by

$$m_{\tilde{\chi}_{1,2}^0} = M_{1,2}, \quad m_{\tilde{\chi}_3^0} = m_{\tilde{\chi}_4^0} = |\mu|. \quad (36)$$

When using the mass-insertion method, one should note the fact that, for any matrix $\mathbf{M} = \mathbf{M}^0 + \mathbf{M}^1$, where $\mathbf{M}^0 = \text{diag}(m_1^0, \dots, m_n^0)$ and \mathbf{M}^1 has no diagonal elements, if the matrix \mathbf{T} can diagonalize the matrix \mathbf{M} , $\mathbf{TMT}^\dagger = \text{diag}(m_1, m_2, \dots, m_n)$, then at leading order for an arbitrary function f we have

$$\mathbf{T}_{ik}^\dagger f(m_k) \mathbf{T}_{kj} = \delta_{ij} f(m_i^0) + \mathbf{M}_{ij}^1 f(m_i^0, m_j^0), \quad (37)$$

with

$$f(x, y, z_1 \dots z_n) = \frac{f(x, z_1 \dots z_n) - f(y, z_1 \dots z_n)}{x - y}. \quad (38)$$

After a straightforward calculation we obtain an analytical expression for the branching ratio

$$\mathcal{B}r(Z \rightarrow \ell_I \bar{\ell}_J) = \frac{\alpha_{\text{em}}^3 c_W^2 m_Z}{48\pi^2 s_W^6 \Gamma_Z} \frac{|\delta(m_L^2)_{IJ}|^2}{M_2^4}$$

$$\begin{aligned} & \times \left| f_1(x_I, x_J) - 2f_2(x_I, x_J) - \frac{\frac{1}{2} + s_W^2}{c_W^2} \frac{f_2\left(\frac{1}{x_I}, \frac{1}{x_J}\right)}{x_I x_J} \right. \\ & \quad \left. + \frac{\frac{1}{2} s_W^2 - s_W^4}{c_W^4} \left(\frac{M_2}{M_1}\right)^2 \left(\frac{f_2\left(\frac{1}{x'_I}, \frac{1}{x'_J}\right)}{x'_I x'_J} - \frac{1}{2} f_3(x'_I, x'_J) \right) \right. \\ & \quad \left. - \frac{3}{2} \frac{\frac{1}{2} - s_W^2}{c_W^2} f_3(x_I, x_J) \right|^2. \end{aligned} \quad (39)$$

Here $s_W = \sin \theta_W$, $c_W = \cos \theta_W$, $x_I = (m_{\tilde{L}}^2)_{II}/M_2^2$, $x'_I = (m_{\tilde{L}}^2)_{II}/M_1^2$, and

$$\begin{aligned} f_1(x) &= \frac{1}{x-1} \left(1 - \frac{x}{x-1} \ln x \right), \\ f_2(x) &= \frac{1}{4(x-1)} \left(1 - \frac{x^2}{x-1} \ln x \right), \\ f_3(x) &= \frac{1}{(x-1)} \left(1 + \frac{x^2 - 2x}{x-1} \ln x \right), \end{aligned} \quad (40)$$

and $f_i(x, y)$ can be obtained through (38).

4 Comparison of LFV Z -decays with lepton decays

Now we compare the LFV Z -decays with lepton decays. Using a similar procedure as in the preceding section, we can easily calculate the decay width for $\ell_J \rightarrow \ell_I \gamma$ by setting $g = e$, $g_{\alpha\beta}^{L,R} = 1$ with $\alpha = \beta$, $G_{XY} = 1$ with $X = Y$ in Fig. 2, and $f_{1L,1R} = 0$ in (24). Meanwhile one should also note the fact that sneutrinos in Fig. 1a and neutralinos in 1b do not couple to the photon and that the self-energy diagrams do not contribute to the dipole operators. The branching ratios of $\ell_J \rightarrow \ell_I \gamma$ are obtained as

$$\frac{\mathcal{B}r(\ell_J \rightarrow \ell_I \gamma)}{\mathcal{B}r(\ell_J \rightarrow \ell_I \nu_J \bar{\nu}_I)} = \frac{6\alpha_{\text{em}} m_W^4}{\pi m_{\ell_J}^2} (|f_{2L}^\gamma|^2 + |f_{2R}^\gamma|^2). \quad (41)$$

Here the form factors are given by [7]

$$f_{2L}^\gamma = \sum_{k=a,b} \frac{1}{m_{\tilde{\chi}_\alpha}^2} C_{I\alpha X}^{*R(k)} \left[m_\alpha C_{J\alpha X}^{L(k)} F_1^k + m_{\ell_J} C_{J\alpha X}^{R(k)} F_2^k \right], \quad (42)$$

$$f_{2R}^\gamma = f_{2L}^\gamma |_{L \leftrightarrow R}, \quad (43)$$

where

$$\begin{aligned} F_1^a(x_a) &= m_{\tilde{\chi}_\alpha^0}^2 (C_0^a + C_{11}^a + C_{12}^a) \\ &= \frac{1}{(x_a - 1)^2} \left(-\frac{x_a + 1}{2} + \frac{x_a}{x_a - 1} \ln x_a \right), \end{aligned} \quad (44)$$

$$F_2^a(x_a) = -m_{\tilde{\chi}_\alpha^0}^2 (C_{12}^a + C_{22}^a + C_{23}^a) \quad (45)$$

$$= \frac{1}{2(x_a - 1)^3} \left(\frac{-x_a^2 + 5x_a + 2}{6} - \frac{x_a}{x_a - 1} \ln x_a \right),$$

$$\begin{aligned} F_1^b(x_b) &= m_{\tilde{\chi}_\alpha^-}^2 (C_{11}^b + C_{12}^b) \\ &= \frac{1}{(x_b - 1)^2} \left(\frac{-3x_b + 1}{2} + \frac{x_b^2}{x_b - 1} \ln x_b \right), \end{aligned} \quad (46)$$

$$F_2^b(x_b) = m_{\tilde{\chi}_\alpha^-}^2 (C_{12}^b + C_{22}^b + C_{23}^b) = \frac{1}{x_b} F_2^a\left(\frac{1}{x_b}\right), \quad (47)$$

with $x_a = m_{\tilde{\ell}_X}^2/m_{\tilde{\chi}_\alpha^0}^2$ and $x_b = m_{\tilde{\nu}_X}^2/m_{\tilde{\chi}_\alpha^-}^2$.

Next we derive the analytical expression for the branching ratios in the limit of $m_S \gg m_Z$. Unlike the form factors for the Z -decays which contain terms not proportional to the small lepton mass [see (25) and (28)], the form factors for $\ell_J \rightarrow \ell_I \gamma$ are always proportional to the small lepton mass m_{ℓ_J} . In this case, the off-diagonal elements in the mass matrices of the chargino and neutralino are no longer negligible, especially when $\tan \beta$ is large. In fact, the terms $m_\alpha C_{I\alpha X}^{*L(b)} C_{J\alpha X}^{R(b)}$ in f_{2R}^γ receive a contribution from the wino-Higgsino mixing, which can be enhanced by $\tan \beta$. So for a large $\tan \beta$, the contribution of f_{2R}^γ is dominant and the branching ratios are given by [2]

$$\begin{aligned} \mathcal{B}r(\ell_J \rightarrow \ell_I \gamma) &\simeq \mathcal{B}r(\ell_J \rightarrow \ell_I \nu_J \bar{\nu}_I) \frac{6\alpha_{\text{em}} m_W^4}{\pi m_{\ell_J}^2} |f_{2R}^\gamma|^2 \\ &= \mathcal{B}r(\ell_J \rightarrow \ell_I \nu_J \bar{\nu}_I) \frac{6\alpha_{\text{em}} m_W^4}{\pi M_2^4} \left(\frac{\mu}{M_2} \right)^2 \\ &\quad \times \left| \frac{1}{2} F_1^a(x_I, x_J) - F_1^b(x_I, x_J) \right. \\ &\quad \left. - \left(\frac{M_2}{\mu} \right)^4 \left(\frac{1}{2} F_1^a(\bar{x}_I, \bar{x}_J) - F_1^b(\bar{x}_I, \bar{x}_J) \right) \right|^2 \\ &\quad \times \frac{|\delta(\mathbf{m}_{\tilde{L}}^2)_{IJ}|^2}{M_2^4} \frac{\tan^2 \beta}{\left(1 - \frac{\mu^2}{M_2^2}\right)^2}, \end{aligned} \quad (48)$$

where $\bar{x}_I = (\mathbf{m}_{\tilde{L}}^2)_{II}/\mu^2$.

Comparing $\mathcal{B}r(\ell_J \rightarrow \ell_I \gamma)$ with $\mathcal{B}r(Z \rightarrow \ell_I \bar{\ell}_J)$, we find the following.

- (1) The dipole transitions in (24), the only operators contributing to $\ell_J \rightarrow \ell_I \gamma$, do not give dominant contributions to the decays $Z \rightarrow \ell_I \bar{\ell}_J$ due to heavy sparticle mass suppression;
- (2) $\mathcal{B}r(Z \rightarrow \ell_I \bar{\ell}_J)$ is not sensitive to $\tan \beta$, whereas $\mathcal{B}r(\ell_J \rightarrow \ell_I \gamma)$ can be enhanced by large $\tan \beta$;
- (3) the ratio $\mathcal{B}r(Z \rightarrow \ell_I \bar{\ell}_J)/\mathcal{B}r(\ell_J \rightarrow \ell_I \gamma)$ is independent of the heavy Majorana sector introduced by the seesaw mechanism.

5 Numerical results

In our numerical calculation we consider the constraints from current neutrino oscillation experiments and the experimental bounds on LFV lepton decays.

Neutrino oscillation experiments

The SK Collaboration [16] showed that the ν_μ created in the atmosphere oscillates into ν_τ with almost maximal mixing, $\sin(2\theta_{\text{atm}}) \sim 1$ and the neutrino mass-square difference is $\Delta m_{\text{atm}}^2 \sim (2-4) \times 10^{-3} \text{ eV}^2$. The second mass-square difference and mixing angle are found to be $\Delta m_{\text{sol}}^2 = (3-15) \times 10^{-5} \text{ eV}^2$, $\sin(2\theta_{\text{sol}}) = 0.7 \sim 0.9$ from solar neutrino experiments [17, 18]. For the third mixing angle, only the upper bound is obtained from the reactor neutrino experiments [19, 20]: $\sin^2 2\theta_{\text{rea}} < 0.1$ for $\Delta m_{\text{atm}}^2 \simeq 3 \times 10^{-3} \text{ eV}^2$.

Although there exists a possibility that neutrino masses are quasi-degenerate, in this work we take the normal mass order $m_{\nu 1} < m_{\nu 2} < m_{\nu 3}$ with values²

$$m_{\nu 1} = 0, \quad m_{\nu 2} = \sqrt{\Delta m_{\text{sol}}^2}, \quad m_{\nu 3} = \sqrt{\Delta m_{\text{atm}}^2}. \quad (49)$$

The mixing angles are fixed to be

$$\theta_{L12} = \theta_{\text{sol}} = 30^\circ, \quad \theta_{L23} = \theta_{\text{atm}} = 45^\circ. \quad (50)$$

Further, we restrict $\theta_{L13} < 10^\circ$. Then $(\mathbf{Y}_\nu^\dagger \mathbf{Y}_\nu)_{IJ}$ in (21) are given by

$$(\mathbf{Y}_\nu^\dagger \mathbf{Y}_\nu)_{12} \simeq \frac{\sqrt{2}}{4v^2 \sin^2 \beta} \left(\frac{\sqrt{3}}{2} m_2^2 + \sin 2\theta_{L13} m_3^2 \right), \quad (51)$$

$$(\mathbf{Y}_\nu^\dagger \mathbf{Y}_\nu)_{13} \simeq \frac{\sqrt{2}}{4v^2 \sin^2 \beta} \left(-\frac{\sqrt{3}}{2} m_2^2 + \sin 2\theta_{L13} m_3^2 \right), \quad (52)$$

$$(\mathbf{Y}_\nu^\dagger \mathbf{Y}_\nu)_{23} \simeq \frac{1}{4v^2 \sin^2 \beta} (2m_2^2 - m_3^2). \quad (53)$$

The dependence of the parameter $\mathbf{Y}_\nu^\dagger \mathbf{Y}_\nu$ on the CP phase δ_L is very weak and thus has been neglected.

Experimental bounds on LFV lepton decays

LFV lepton decays have been searched in several experiments and the current bounds are given by [22–25]

$$\mathcal{B}r(\mu \rightarrow e\gamma) < 1.2 \times 10^{-11}, \quad (54)$$

$$\mathcal{B}r(\tau \rightarrow (e, \mu)\gamma) < (2.7, 1.1) \times 10^{-6}, \quad (55)$$

$$\mathcal{B}r(Z \rightarrow \tau\bar{\mu}) < 1.2 \times 10^{-5}, \quad (56)$$

$$\mathcal{B}r(Z \rightarrow (\mu, \tau)\bar{e}) < (1.7, 9.8) \times 10^{-6}. \quad (57)$$

In addition, the explanation of the observed lepton number asymmetry by the seesaw mechanism gives a lower bound for the heavy Majorana neutrinos of $\mathcal{M}_1 > 10^{11} \text{ GeV}$ [12]. Considering the constraints mentioned above and fixing the right-handed neutrino masses as $\mathcal{M}_1 = 10^{13} \text{ GeV}$, $\mathcal{M}_2 \simeq 10^{15} \text{ GeV}$, we solve the full RG equations listed in

² In general, the impact of RG evolution on neutrino masses and mixing angles can be large; however, it is small for the hierarchy of neutrinos we chose [21]

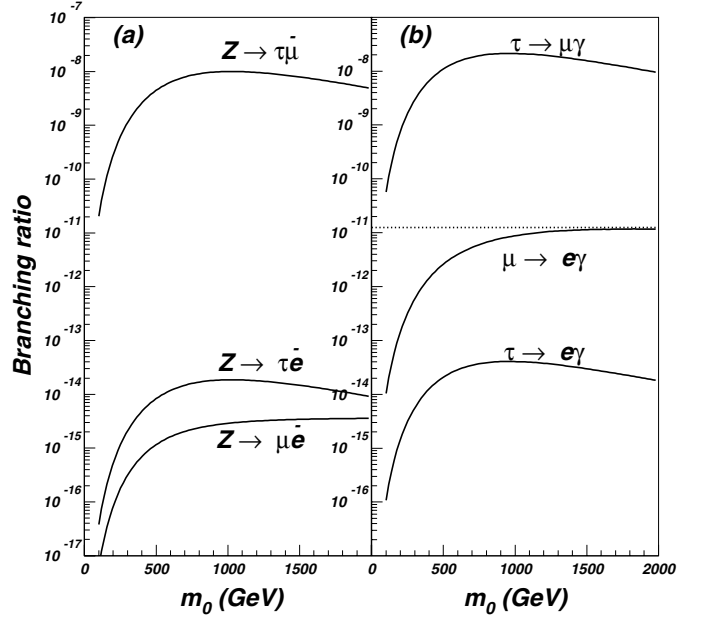


Fig. 3a,b. Branching ratios of $Z \rightarrow \ell_I \bar{\ell}_J$ and $\ell_J \rightarrow \ell_I \gamma$ versus the common scalar mass m_0 . Other parameters are fixed to be $m_{1/2} = 800 \text{ GeV}$, $A_0 = 0$, $\tan \beta = 10$, $m_2 = 10 \text{ GeV}$, $m_3/m_2 = 30$ and $\theta_{L13} = 0$. The dashed line in (b) is the experimental upper bound on $\mu \rightarrow e\gamma$

Appendix A numerically based on the work of [26], where the experimental bounds from $b \rightarrow s\gamma$ and $g_\mu - 2$ have already been taken into account. Although the processes $Z \rightarrow \ell_I \bar{\ell}_J$ are closely correlated to $\ell_J \rightarrow \ell_I \gamma$ and there is a quite stringent bound on $\mu \rightarrow e\gamma$, our numerical results show that there exists a scenario with $m_2 \ll m_3$ and a very small θ_{L13} , in which a large branching ratio for $Z \rightarrow \tau\bar{\mu}$ is obtained.

In Fig. 3 we show the branching ratios of $Z \rightarrow \ell_I \bar{\ell}_J$ and $\ell_J \rightarrow \ell_I \gamma$ versus the common scalar mass m_0 . From Fig. 3 we have the following observations.

(1) With fixed $m_{1/2}$ and $\tan \beta$, both $\mathcal{B}r(Z \rightarrow \tau\bar{\mu})$ and $\mathcal{B}r(\tau \rightarrow \mu\gamma)$ reach their maximum values as $m_0 \simeq 1000 \text{ GeV}$ and then drop slowly as m_0 gets larger.

(2) The branching ratio of $Z \rightarrow \tau\bar{\mu}$ can be as large as 10^{-8} .

Since 5.5×10^9 Z -bosons will be produced at the LHC [9] and the possible sensitivity of GigaZ to $Z \rightarrow \tau\bar{\mu}$ will be up to 10^{-8} [10], the mode $Z \rightarrow \tau\bar{\mu}$ will be accessible at both the LHC and TESLA GigaZ. It is noticeable that the branching ratios are sensitive to the mixing angle θ_{L13} except for the processes $Z \rightarrow \tau\bar{\mu}$ and $\tau \rightarrow \mu\gamma$. As an illustration, we plot the dependence on θ_{L13} in Fig. 4. We see that to satisfy the experimental constraint on $\mu \rightarrow e\gamma$, the mixing angle θ_{L13} must be quite small. Therefore, joint measurements for LFV Z -decays and lepton decays will set strong constraints on the model parameter space.

6 Conclusions

We evaluated the lepton flavor violation Z -decays in the framework of the supersymmetric seesaw model for the

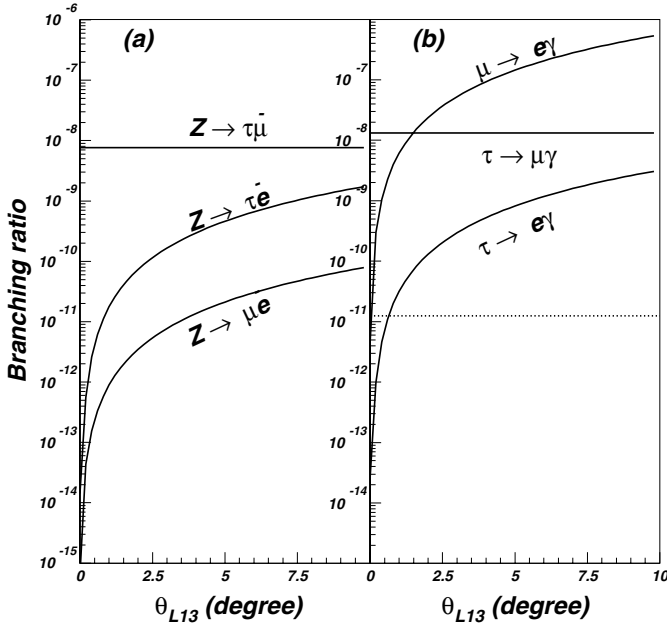


Fig. 4a,b. Same as Fig. 3, but versus the mixing angle θ_{L13} with $m_0 = 500$ GeV

first time. Although different forms of neutrino couplings may lead to different sizes of LFV Z -decays, we emphasize that it is important to study how large the rate for the LFV can be for some typical cases and analyze the possibility to observe $Z \rightarrow \ell_I \bar{\ell}_J$ in future experiments. From our calculational results we conclude that, subject to the constraints from the existing neutrino oscillation data and the experimental bounds on the decays $\ell_J \rightarrow \ell_I \gamma$, the LFV Z -decays $Z \rightarrow \ell_I \bar{\ell}_J$ can still be sizable in the supersymmetric seesaw model, among which the largest-rate channel $Z \rightarrow \tau \bar{\mu}$ can occur with a branching ratio of 10^{-8} and thus may be accessible at the LHC and GigaZ experiment.

Acknowledgements. We thank T. Morozumi, J.I. Illnan and C. Grosche for very useful discussions and comments. The work of Z. Xiong was supported by the Grant-in-Aid for JSPS Fellows (No. 1400230400).

A Renormalization group equations in SUSY seesaw model

In this appendix we present *additional* contributions to the RG equations of some parameters in the supersymmetric seesaw model due to non-zero neutrino interactions. A detailed description of these equations can be found in [1,2]. At one-loop level, the RG equations are given as follows.

(1) For Yukawa couplings:

$$\frac{d\mathbf{Y}_\nu}{dt} = \frac{\mathbf{Y}_\nu}{16\pi^2} \left(T_2 - g_1^2 - 3g_2^2 + 3\mathbf{Y}_\nu^\dagger \mathbf{Y}_\nu + \mathbf{Y}_\ell^\dagger \mathbf{Y}_\ell \right), \quad (58)$$

$$\frac{d\mathbf{Y}_\ell}{dt} = \frac{\mathbf{Y}_\ell}{16\pi^2} \mathbf{Y}_\nu^\dagger \mathbf{Y}_\nu, \quad (59)$$

$$\frac{d\mathbf{Y}_U}{dt} = \frac{\mathbf{Y}_U}{16\pi^2} \text{Tr}(\mathbf{Y}_\nu^\dagger \mathbf{Y}_\nu), \quad (60)$$

where $t = \ln \mu_r$ with μ_r being the renormalization scale, and $T_2 = \text{Tr}(3\mathbf{Y}_U^\dagger \mathbf{Y}_U + \mathbf{Y}_\nu^\dagger \mathbf{Y}_\nu)$. \mathbf{Y}_U is the Yukawa coupling matrix for up-type quarks, and g_1, g_2 and g_3 are the $U(1)_Y$, $SU(2)$ and $SU(3)$ gauge coupling constants, respectively.

(2) For soft parameters:

$$\begin{aligned} \frac{d\mathbf{m}_L^2}{dt} = \frac{1}{16\pi^2} & \left[\mathbf{m}_L^2 \mathbf{Y}_\nu^\dagger \mathbf{Y}_\nu + \mathbf{Y}_\nu^\dagger \mathbf{Y}_\nu \mathbf{m}_L^2 + 2\mathbf{Y}_\nu^\dagger \mathbf{m}_\nu^2 \mathbf{Y}_\nu \right. \\ & \left. + 2m_{H_2}^2 \mathbf{Y}_\nu^\dagger \mathbf{Y}_\nu + 2\mathbf{A}_\nu^\dagger \mathbf{A}_\nu \right], \quad (61) \end{aligned}$$

$$\begin{aligned} \frac{d\mathbf{m}_\nu^2}{dt} = \frac{1}{8\pi^2} & \left[\mathbf{m}_\nu^2 \mathbf{Y}_\nu \mathbf{Y}_\nu^\dagger + \mathbf{Y}_\nu \mathbf{Y}_\nu^\dagger \mathbf{m}_\nu^2 + 2\mathbf{Y}_\nu \mathbf{m}_L^2 \mathbf{Y}_\nu^\dagger \right. \\ & \left. + 2m_{H_2}^2 \mathbf{Y}_\nu \mathbf{Y}_\nu^\dagger + 2\mathbf{A}_\nu \mathbf{A}_\nu^\dagger \right], \quad (62) \end{aligned}$$

$$\begin{aligned} \frac{dm_{H_2}^2}{dt} = \frac{1}{8\pi^2} & \text{Tr} \left[\mathbf{Y}_\nu^\dagger \left(\mathbf{m}_L^2 + \mathbf{m}_\nu^2 + m_{H_2}^2 \right) \mathbf{Y}_\nu + \mathbf{A}_\nu^\dagger \mathbf{A}_\nu \right], \quad (63) \end{aligned}$$

$$\frac{d\mathbf{A}_\ell}{dt} = \frac{1}{16\pi^2} \left(2\mathbf{Y}_\ell \mathbf{Y}_\nu^\dagger \mathbf{A}_\nu + \mathbf{A}_\ell \mathbf{Y}_\nu^\dagger \mathbf{Y}_\nu \right), \quad (64)$$

$$\begin{aligned} \frac{d\mathbf{A}_\nu}{dt} = \frac{1}{16\pi^2} & \left\{ [T_2 - g_1^2 - 3g_2^2 + 4\mathbf{Y}_\nu \mathbf{Y}_\nu^\dagger] \mathbf{A}_\nu + \mathbf{A}_\nu \mathbf{Y}_\ell^\dagger \mathbf{Y}_\ell \right. \\ & \left. + [2\text{Tr} \left(3\mathbf{Y}_U^\dagger \mathbf{A}_U + \mathbf{Y}_\nu^\dagger \mathbf{A}_\nu \right) + 5\mathbf{A}_\nu \mathbf{Y}_\nu^\dagger] \mathbf{Y}_\nu \right. \\ & \left. - 2(g_1^2 M_1 + 3g_2^2 M_2) \mathbf{Y}_\nu + 2\mathbf{Y}_\nu \mathbf{Y}_\ell^\dagger \mathbf{A}_\ell \right\}. \quad (65) \end{aligned}$$

(3) For neutrino masses [27]:

$$\frac{d\mathbf{M}}{dt} = \frac{1}{8\pi^2} \left[\mathbf{M}(\mathbf{Y}_\nu \mathbf{Y}_\nu^\dagger)^T + \mathbf{Y}_\nu \mathbf{Y}_\nu^\dagger \mathbf{M} \right], \quad (66)$$

$$\begin{aligned} \frac{d\mathbf{M}_\nu}{dt} = \frac{1}{16\pi^2} & \left\{ [2T_2 + (\mathbf{Y}_\nu^\dagger \mathbf{Y}_\nu + \mathbf{Y}_\ell^\dagger \mathbf{Y}_\ell)^T] \mathbf{M}_\nu \right. \\ & \left. + \mathbf{M}_\nu \left(\mathbf{Y}_\nu^\dagger \mathbf{Y}_\nu + \mathbf{Y}_\ell^\dagger \mathbf{Y}_\ell - 2g_1^2 - 6g_2^2 \right) \right\}. \quad (67) \end{aligned}$$

Note that the above RG equations are valid for the running from M_P to M . Below the scale M , the RG equations are the same except that the couplings of the right-handed neutrinos do not appear.

References

1. J.A. Casas, A. Ibarra, Nucl. Phys. B **618**, 171 (2001)
2. J. Hisano, T. Moroi, K. Tobe, M. Yamaguchi, Phys. Lett. B **357**, 579 (1995); Phys. Lett. B **391**, 341 (1997); Phys. Rev. D **53**, 2442 (1996); J. Hisano, D. Nomura, Phys. Rev. D **59**, 116005 (1999); J. Hisano et al., Phys. Rev. D **58**, 116010 (1998); J. Hisano, D. Nomura, T. Yanagida, Phys. Lett. B **437**, 351 (1998)
3. J. Ellis et al., Eur. Phys. J. C **14**, 319 (2000); M.E. Gomez, G.K. Leontaris, S. Lola, J.D. Vergados, Phys. Rev. D **59**, 116009 (1999); J.L. Feng, Y. Nir, Y. Shadmi, Phys. Rev.

- D **61**, 113005 (2000); G.K. Leontaris, N.D. Tracas, Phys. Lett. B **431**, 90 (1998); W. Buchmuller, D. Delepine, L.T. Handoko, Nucl. Phys. B **576**, 445 (2000); W. Buchmuller, D. Delepine, F. Vissani, Phys. Lett. B **459**, 171 (1999); J. Sato, K. Tobe, Phys. Rev. D **63**, 116010 (2001); J. Sato, K. Tobe, T. Yanagida, Phys. Lett. B **498**, 189 (2001); D.F. Carvalho, M.E. Gomez, S. Khalil, JHEP **0107**, 001 (2001); S.F. King, M. Oliveira, Phys. Rev. D **60**, 035003 (1999); R. Barbieri, L.J. Hall, A. Strumia, Nucl. Phys. B **445**, 219 (1995)
4. M. Frank, H. Hamidian, Phys. Rev. D **54**, 6790 (1996)
 5. D.F. Carvalho, M.E. Gómez, J.C. Romao, Phys. Rev. D **65**, 093013 (2002)
 6. D. Atwood, S. Bar-Shalom, G. Eilam, A. Soni, Phys. Rev. D **66**, 093005 (2002)
 7. J.I. Illana, M. Masip, Phys. Rev. D **67**, 035004 (2003); J.I. Illana, T. Riemann, Phys. Rev. D **63**, 053004 (2001)
 8. A.H. Chamseddine, R. Arnowitt, P. Nath, Phys. Rev. Lett. **49**, 970 (1982); R. Barbieri, S. Ferrara, C.A. Savoy, Phys. Lett. B **119**, 343 (1982); L.J. Hall, J. Lykken, S. Weinberg, Phys. Rev. D **27**, 2359 (1983)
 9. A.D. Martin et al., Eur. Phys. J. C **14**, 133 (2000)
 10. J.A. Aguilar-Saavedra et al. (ECFA/DESY LC physics Working Group), hep-ph/0106315
 11. T. Yanagida, Prog. Theor. Phys. **64**, 1103 (1980); R.N. Mohapatra, G. Senjanovic, Phys. Rev. Lett. **44**, 912 (1980)
 12. T. Endoh, S. Kaneko, S.K. Kang, T. Morozumi, M. Tanimoto, Phys. Rev. Lett. **89**, 231601 (2002) [hep-ph/0209020]
 13. Z. Maki, M. Nakagawa, S. Sakata, Prog. Theor. Phys. **28**, 870 (1962)
 14. H.E. Haber, G.L. Kane, Phys. Rep. **117**, 75 (1985); J.F. Gunion, H.E. Haber Nucl. Phys. B **272**, 1 (1986)
 15. G. 't Hooft, M. Veltman, Nucl. Phys. B **153**, 365 (1979); G. Passarino, M. Veltman, Nucl. Phys. B **160**, 151 (1979)
 16. For a review, see C.K. Jung, C. McGrew, T. Kajita, T. Mann, Ann. Rev. Nucl. Part. Sci. **51**, 451 (2001)
 17. SNO Collaboration, Q.R. Ahmad et al., Phys. Rev. Lett. **89**, 011301, 011302 (2002)
 18. KamLAND Collaboration, K. Eguchi et al., Phys. Rev. Lett. **90**, 021802 (2003)
 19. The CHOOZ Collaboration, Phys. Lett. B **420**, 397 (1998)
 20. F. Boehm, et al., Phys. Rev. Lett. **84**, 3764 (2000); Phys. Rev. D **62**, 072002 (2000); **64**, 112001 (2001)
 21. See, for example, J.A. Casas, J.R. Espinosa, A. Ibarra, I. Navarro, Nucl. Phys. B **573**, 652 (2000)
 22. MEGA Collaboration, M.L. Brooks et al., Phys. Rev. Lett. **83**, 1521 (1999)
 23. CLEO Collaboration, K.W. Edwards et al., Phys. Rev. D **55**, 3919 (1997); S. Ahmed et al., Phys. Rev. D **61**, 071101 (2000)
 24. OPAL Collaboration, R. Akers et al., Z. Phys. C **67**, 555 (1995)
 25. DELPHI Collaboration, P. Abreu et al., Z. Phys. C **73**, 243 (1997)
 26. A. Djouadi, J.-L. Kneur, G. Moultaka, hep-ph/0211331
 27. S. Antusch, J. Kersten, M. Lindner, M. Ratz, Phys. Lett. B **538**, 87 (2002)